Point Defect Engineering of High-Performance Bismuth-Telluride-Based Thermoelectric Materials

Lipeng Hu, Tiejun Zhu, Xiaohua Liu, and Xinbing Zhao**

Developing high-performance thermoelectric materials is one of the crucial aspects for direct thermal-to-electric energy conversion. Herein, atomic scale point defect engineering is introduced as a new strategy to simultaneously optimize the electrical properties and lattice thermal conductivity of thermoelectric materials, and $(Bi,Sb)_2(Te,Se)_3$ thermoelectric solid solutions are selected as a paradigm to demonstrate the applicability of this new approach. Intrinsic point defects play an important role in enhancing the thermoelectric properties. Antisite defects and donor-like effects are engineered in this system by tuning the formation energy of point defects and hot deformation. As a result, a record value of the figure of merit *ZT* of ≈1.2 at 445 K is obtained for n-type polycrystalline $Bi_2Te_{2.3}Se_{0.7}$ alloys, and a high *ZT* value of ≈1.3 at 380 K is achieved for p-type polycrystalline $Bi_{0.3}Sb_{1.7}Te_3$ alloys, both values being higher than those of commercial zone-melted ingots. These results demonstrate the promise of point defect engineering as a new strategy to optimize thermoelectric properties.

1. Introduction

Thermoelectric (TE) coolers and generators have attracted extensive interest in the past decades due to various promising properties: direct conversion between heat and electricity, vibration-free operation, high reliability, and low environmental impact. The conversion efficiency of TE devices depends on the dimensionless figure of merit *ZT* of the materials, $ZT = \sigma\alpha^2 T/\kappa$, where T is the operating temperature, and the interdependent TE parameters α, σ, and κ are the Seebeck coefficient, the electrical conductivity, and the thermal conductivity (including the lattice contribution κ_{ph} and the carrier contribution κ_{el}), respectively. Two main strategies have recently been adopted to obtain high-performance TE materials, namely phonon engineering[1–5] and band engineering,[6,7] which are used separately to optimize the thermal and electronic transport properties. For example, incorporation of nanostructures into bulk TE materials as phonon scattering centers is an effective approach to minimize κ_{ph} and to improve *ZT*.[1] An alternative approach to increase *ZT* is to enhance the power factor ($PF = \sigma\alpha^2$) by band structure modification, such as tuning of resonant levels[6] or band convergence.[7]

The decoupling of interdependent TE parameters has been a longstanding challenge because they are strongly coupled by the carrier concentration.[8] Here, we propose atomic scale point defect engineering as one new possible solution that can simultaneously optimize the electrical properties and lattice thermal conductivity. Point defects play an important role in TE transport. For example, Mg interstitials in $Mg_2(Si,Sn)$ TE solid solutions increase the carrier concentration,[9] while Mg vacancies, which act as additional phonon scattering centers, can reduce the lattice thermal conductivity κ_{ph}.[10] Point defects also change the band structure. Theoretical calculations demonstrated that in ZrNiSn based half-Heusler TE alloys the bandgap decreases with increasing Zr/Sn antisite defect content.[11]

In $(Bi,Sb)_2(Te,Se)_3$ based alloys, the best TE materials near room temperature, inherent point defects occur during the crystal growth from the stoichiometric melt. Negatively charged antisite defects such as Sb'_{Te}, Bi'_{Te}, and Bi'_{Te} are formed when excess cation atoms occupy the vacant anion sites, which accounts for the p-type conductivity.[12] On the other hand, the anion vacancies ($V^{\cdot\cdot}_{Te}$ and $V^{\cdot\cdot}_{Se}$) carrying positive charges are generated if the empty anion sites are retained, which is compensated by electrons.[13] Recently, the existence of these native defects has been directly confirmed by scanning tunnelling microscopy.[14] However, the important role of point defects is generally ignored in recent TE research, especially for Bi_2Te_3 based alloys with inherent antisite defects or vacancies. In this work, point defect engineering is proposed as a new and effective approach to enhance the TE performance, and $(Bi,Sb)_2(Te,Se)_3$ solid solutions are selected as a paradigm to demonstrate the applicability of this new strategy.

The concentration of antisite defects or vacancies in bismuth telluride based solid solutions strongly depends on the composition. The smaller the differences in electronegativity χ and atomic size between the cation and anion atoms, the less resistance to the formation of antisite defects.[12] Nevertheless, by increasing the size difference between the cation and anion atoms, anion vacancies form more readily.[13] The basic properties of these constituent elements in Bi_2Te_3 based alloys are summarized in Table S1 (Supporting Information). The

L. P. Hu, Prof. T. J. Zhu, X. H. Liu, Prof. X. B. Zhao
State Key Laboratory of Silicon Materials
Department of Materials Science and Engineering
Zhejiang University
Hangzhou 310027, China
E-mail: zhutj@zju.edu.cn; zhaoxb@zju.edu.cn
Prof. T. J. Zhu, Prof. X. B. Zhao
Key Laboratory of Advanced Materials and Applications for Batteries of Zhejiang Province
Zhejiang University
Hangzhou 310027, China

DOI: 10.1002/adfm.201400474

© 2014 WILEY-VCH Verlag GmbH & Co. KGaA, Weinheim

formation energy of antisite defects E_{AS} can be enumerated in ascending order:

$$E_{AS}(\text{Sb–Te}) < E_{AS}(\text{Bi–Te}) < E_{AS}(\text{Sb–Se}) < E_{AS}(\text{Bi–Se}) \quad (1)$$

The formation energy of anion vacancies E_V is listed in descending order:

$$E_V(\text{Sb–Te}) < E_V(\text{Bi–Te}) < E_V(\text{Sb–Se}) < E_V(\text{Bi–Se}) \quad (2)$$

This simple defect model permits us to qualitatively predict the conduction type and accounts for the carrier concentration variation with composition. In the binary systems, undoped Sb_2Te_3 alloys exhibit very strong p-type characteristics, while Bi_2Te_3 alloys are weakly p-type, which is due to the larger difference in χ and atomic size in the latter. Similarly, the low E_V value demonstrates the strong n-type behavior of the binary Bi_2Se_3 alloy. This defect model has recently been corroborated by first-principles calculations that consider spin-orbit interaction.[14]

It is necessary to mention that excess electrons can be introduced into the lattice by the deformation-induced donor-like effect, which significantly changes the carrier concentration.[15] Typically, unidirectionally grown Bi_2Te_3 based alloys with a maximum $ZT \approx 1$ exhibit poor mechanical properties due to the weak van der Waals bonding between $Te^{(1)}$–$Te^{(1)}$ layers in the rhombohedral crystal structure. In recent years, a combination of ball milling (BM) and hot pressing (HP) has been used to improve the mechanical properties and to reduce κ_{ph} by enhancing boundary scattering of phonons.[1] However, the impact of deformation-induced donor-like effects on the TE properties has been ignored in many recent studies.[1,2,16] Recently, we found that hot deformation (HD) also leads to the donor-like effect.[8,17] Deformation induces the non-basal slip and produces, on average, 3 Te to 2 Bi vacancy-interstitial pairs.[18] When abundant Bi vacancies are created, the Bi atoms occupying the Te sites would more readily diffuse back into its original sublattices and excess Te vacancies are thereupon produced:[15]

$$2V_{Bi}^{'''} + 3V_{Te}^{\cdot\cdot} + Bi_{Te}^{'} \rightarrow V_{Bi}^{'''} + Bi_{Bi}^{\times} + 4V_{Te}^{\cdot\cdot} + 6e' \quad (3)$$

where $V_{Bi}^{'''}$ and $V_{Te}^{\cdot\cdot}$ are the Bi and Te vacancies generated from the deformation process, $Bi_{Te}^{'}$ is the antisite defect formed during the crystal growth, and e′ is an excess electron. An analogous formula is valid for $V_{Sb}^{'''}$, $Sb_{Te}^{'}$, $Bi_{Se}^{'}$ and $V_{Se}^{\cdot\cdot}$. The excess anion vacancies (i.e., $V_{Te}^{\cdot\cdot}$ and $V_{Se}^{\cdot\cdot}$) that were created by the deformation induced non-basal slip are hereafter denoted as donor-like defects. It is clear that the donor-like effect depends on two factors: antisite defects and the deformation induced vacancies.

As aforementioned, the interrelated thermoelectric parameters are all highly dependent on the carrier concentration. Although the effect of point defects on the carrier concentration of Bi_2Te_3 based alloys has been reported, there are few studies on how to utilize point defects to design and optimize compositions and to improve TE properties of polycrystalline Bi_2Te_3 alloys. Furthermore, point defects reduce κ_{ph} by scattering phonons due to either mass contrast or local strains. Theoretically, κ of Bi_2Te_3 alloys can be decreased down to 60–70% by bismuth or tellurium vacancies and about 20% by antisite defects.[19] In this work, a hot deformation approach is used to engineer point defects, and an enhancement of ZT for both n- and p-type ternary Bi_2Te_3-based polycrystalline alloys is realized. A record ZT value of ≈1.2 for n-type polycrystalline Bi_2Te_3 is obtained with the thermal and electrical properties being measured along the same direction. The present results strongly demonstrate the efficacy of point defect engineering and provide a new route for improving TE properties.

2. Results and Discussion

2.1. Ternary n-Type $Bi_2Te_{3-x}Se_x$ System

To construct a fully functioning optimal TE generator, both n- and p-type materials with similar performance are needed. Despite high ZT values of ≈1.3 have been achieved for p-type polycrystalline Bi_2Te_3 based alloys by nanostructuring,[1,2,20] the maximum ZT value of n-type alloys is only close to unity.[8,16,17] Thus, obtaining high efficiency n-type alloys that match well with p-type counterparts is a great challenge.

Figure 1a shows the room temperature carrier concentration n_H of undoped single crystal and polycrystalline $Bi_2Te_{3-x}Se_x$

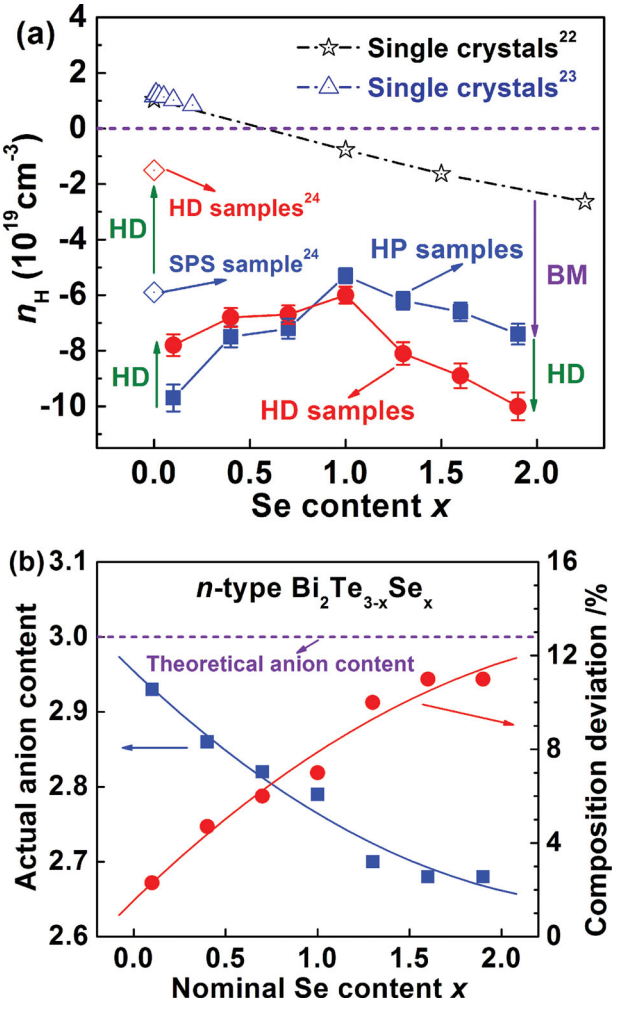

Figure 1. a) Room temperature carrier concentration of the undoped single crystals,[22,23] HP and HD $Bi_2Te_{3-x}Se_x$ samples, and literature data.[24] b) Actual compositions analyzed by electron probe microanalysis (EPMA) of the polycrystalline $Bi_2Te_{3-x}Se_x$ samples.

© 2014 WILEY-VCH Verlag GmbH & Co. KGaA, Weinheim

samples. The latter was obtained by ball milling, hot pressing and hot deformation. According to the above described point defect model, the substitution of Te sites by Se in weakly p-type Bi_2Te_3 single crystals increases E_{AS} and decreases E_V due to the greater difference of χ and size in Bi–Se as compared to Bi–Te (Table S1, Supporting Information). The concentration of anion vacancies ($V_{Te}^{\cdot\cdot}$ and $V_{Se}^{\cdot\cdot}$) gradually surpasses that of antisite defects ($Bi_{Te}^{'}$ and $Bi_{Se}^{'}$), which induces a p-n type transition in the undoped single crystals of $Bi_2Te_{3-x}Se_x$ with increasing Se content. Unidirectionally grown $Bi_2Te_{3-x}Se_x$ ingots have optimal matrix compositions at $x = 0.15 - 0.3$, thereby showing weak p-type conduction because the dominant point defects are antisite defects at these compositions. Donor doping with expensive halide is generally applied to realize the p-n transition and to optimize the electron concentration to $\approx 5 \times 10^{19}$ cm^{-3}.[21] Alternatively, the p-n transition at these compositions could be caused by the deformation induced donor-like effect. Figure 1a shows that the donor-like effect provides high electron concentrations, which results in n-type conductivity for all the polycrystalline samples subjected to BM (HP and HD samples), especially at the typical optimum compositions ($x = 0.15 - 0.3$). Thus, a reassessment of the optimum composition for polycrystalline $Bi_2Te_{3-x}Se_x$ subjected to mechanical deformation is required.

The room temperature carrier concentration n_H of the polycrystalline HD and HP samples firstly falls and then rises with increasing the Se content x (Figure 1a), which can be clearly explained by the concept of point defects. The electron concentration of the HP samples results from both inherent anion vacancies and the deformation-induced donor-like effect. However, the anion vacancies are ever-rising with increasing x, which cannot explain the reduction of n_H at $x < 1.0$. A similar result has also been observed in a previous report.[24] The degree of donor-like effect mainly depends on the concentration of antisite defects under the same deformation conditions according to Equation (3). The electron concentration produced by the donor-like effect decreases with increasing x because of the initial decrease in antisite defects. Thus, the optimum composition of the polycrystalline n-type alloys is $x = 0.7 - 1.0$ with a suppressed donor-like effect and n_H of $\approx 5–6 \times 10^{19}$ cm^{-3} (Figure 1a). When the Se content is further increased to $x > 1$, however, n_H increases again. In addition to the increased anion vacancies, this might result from the re-enhanced donor-like effect, because the concentration of antisite defects rises at $x > 1$. The antisite defect concentration is the consequence of E_{AS} and the overstoichiometry of cation atoms. Because Se is volatilized more readily than Te, there will be more excess Bi atoms with increasing x, as demonstrated in Figure 1b. Both E_{AS} and the excess Bi atoms increase with x, which has a contrary effect on the antisite defect concentration, leading to a "down-up" variation trend for the antisite defects. Indeed, despite the strong n-type conduction, the concentration of $Bi_{Se}^{'}$ antisite defects in Bi_2Se_3 crystals ($\approx 4 \times 10^{19}$ cm^{-3}) is higher than that of $Bi_{Te}^{'}$ in Bi_2Te_3 ($\approx 1 \times 10^{19}$ cm^{-3}).[13]

Note that the HD samples have a lower n_H than the HP counterparts with low Se contents but a higher n_H at $x \geq 1.0$ (Figure 1a). Hot deformation is an effective method to further tune the point defects and to improve the TE performance.[8,17] Different from the sole donor-like effect during the ball milling of the HP samples, both donor-like effects and recovery coexist in the HD process. The antisite defects are nearly depleted by the BM-induced donor-like effect for the HP samples with low contents of Se. Thus, the donor-like effect cannot further occur in the subsequent HD process. Our previous studies indicate that raising the hot deformation temperature or annealing will mitigate donor-like defects (i.e., $V_{Te}^{\cdot\cdot}$ and $V_{Se}^{\cdot\cdot}$) due to the recovery effect,[8,17] and results in the reduction of n_H. A similar phenomenon was reported by Zhao et al.[24] They pointed out that n_H of samples fabricated by spark plasma sintering (SPS) is lower than that of HD counterparts for the pure Bi_2Te_3 bulk because of the recovery role (Figure 1a). On the contrary, at high Se contents with higher concentration of antisite defects, only a part of the antisite defects contributes to the donor-like effect caused by BM, and the donor-like effect is further provoked during HD.[8,17] This leads to higher electron concentrations ($>6 \times 10^{19}$ cm^{-3}) than in the HP counterparts, indicating that samples of high Se-content are not suitable as good n-type Bi_2Te_3 based materials.

By optimizing n_H via engineering point defects instead of doping, good electrical properties can be obtained. The initial decrease of σ for HD samples with increasing x in **Figure 2**a and b is mainly ascribed to the decrease of n_H. The minimum σ at room temperature is $\approx 1.2 \times 10^5$ Sm^{-1} for hot deformed Bi_2Te_2Se. Raising the Se content to $x > 1$, σ dramatically increases due to the increase of n_H. The HD samples showed a higher σ value for the whole range of Se content even though n_H is lower than that of the HP counterparts at low Se contents, which is ascribed to the higher μ_H value of the former. Hot deformation could enhance the texture to some extent and hence improve the carrier mobility μ_H.[8,16,17,24] The in-plane X-ray diffraction patterns of the HP and HD samples show that the (00l) diffraction intensities of the HD sample are much higher than that of the HP counterpart, revealing the formation of texture (Figure S1, Supporting Information). Thus, μ_H of the HD polycrystalline samples is higher than that of the HP counterparts (Figure S1, Supporting Information). Figure 2c,d show that the absolute value of α for polycrystalline samples first slightly rises and then falls, contrary to σ. Figure 2e,f show that the power factor PF of polycrystalline samples monotonously declines with increasing the Se content. Besides, the HD samples have an improved PF for all the compositions compared to the HP counterparts. It should be noted that all the TE parameters were measured along the growth direction of the single crystals and the in-plane direction for the polycrystalline HP and HD samples.

Point defects also have a significant influence on κ. The κ value of polycrystalline $Bi_2Te_{3-x}Se_x$ samples firstly drops and then rises with increasing x, which is in accordance with the variation of σ (**Figure 3**a,b). Compared with the HP samples, the HD counterparts show a higher κ value, mainly due to a higher κ_{el}, which is consistent with results by Zhao et al.[24] The minimum κ value was obtained at $x = 0.7$. κ_{ph} of the HD samples in Figure 3c was estimated by subtracting κ_{el} from κ, where κ_{el} was calculated using the Wiedemann-Franz law with $L_0 = 2.0 \times 10^{-8}$ V^{2}K^{-2}. The anomalous rise of κ_{ph} at

© 2014 WILEY-VCH Verlag GmbH & Co. KGaA, Weinheim

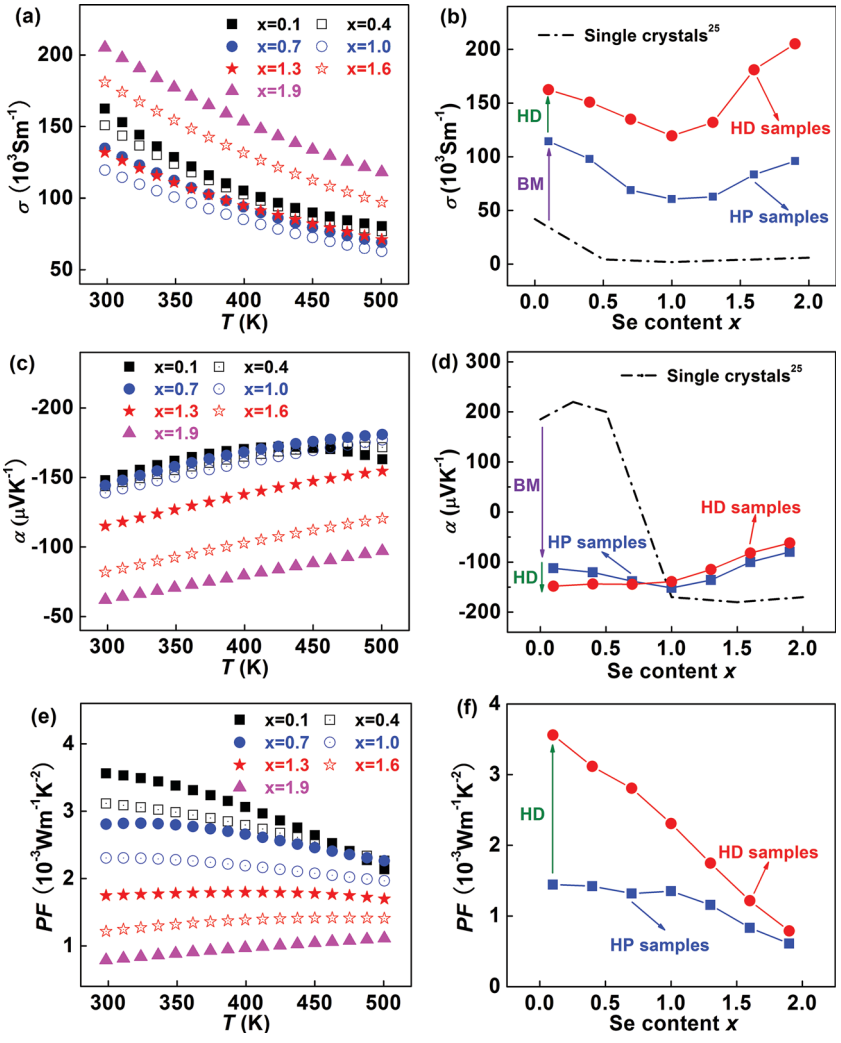

Figure 2. a) Temperature dependence of in-plane electrical conductivity of the hot deformed $Bi_2Te_{3-x}Se_x$ samples. b) Room temperature electrical conductivity of the single crystals,[25] HP and HD $Bi_2Te_{3-x}Se_x$ samples. c) Temperature dependence of the Seebeck coefficient of the hot deformed $Bi_2Te_{3-x}Se_x$ samples. d) Room temperature Seebeck coefficient of the single crystals,[25] HP and HD $Bi_2Te_{3-x}Se_x$ samples. e) Temperature dependence of the power factor of the hot deformed $Bi_2Te_{3-x}Se_x$ samples. f) Room temperature power factor of the HP and HD $Bi_2Te_{3-x}Se_x$ samples.

x = 1.0 – 1.5 is a result of atom ordering (Figure 3d).[26] Both antisite defects and vacancies contribute to the reduction of κ_{ph}, but the effect of vacancies is much greater because of the larger mass and size differences between the occupied sites and the vacancies. The deformation induced vacancies V_{Bi}''' and $V_{Te}^{\cdot\cdot}$ (or $V_{Se}^{\cdot\cdot}$) in the HD samples further scatter the phonons and reduce κ_{ph} (Figure 3d). In addition, high-density lattice defects such as the lattice distortions and dislocations generated during the HD process also contribute to the reduction of κ_{ph}.[8,17,20]

By engineering the point defects via tuning the Se content and hot deformation, the hot deformed $Bi_2Te_{2.3}Se_{0.7}$ sample exhibits a ZT value of ≈1.0 at 500 K (**Figure 4**a). Different from the typically zone-melted (ZM) alloys with x = 0.15 – 0.3,[21,26] the optimum compositions of the polycrystalline samples are shifted to a higher Se content of x = 0.7 (Figure 4b), because the donor-like effect will significantly increase the electron concentration. More importantly, there is a significant improvement of the average ZT_{av} value throughout the entire temperature range studied, which is 0.87 for the $Bi_2Te_{2.3}Se_{0.7}$ HD sample (Figure S2, Supporting Information). In order to corroborate the reproducibility, the $Bi_2Te_{2.3}Se_{0.7}$ sample has been re-prepared twice using the same procedure and repeatable ZT values have been obtained (Figure S2, Supporting Information).

To further improve the ZT value of the $Bi_2Te_{2.3}Se_{0.7}$ alloy, its electrical properties need to be optimized. In our previous work, repetitive hot deformation has been successfully employed to obtain high-performance n-type $Bi_2Te_2Se_1$ alloys.[17] Here the same procedure was implemented for the optimized composition $Bi_2Te_{2.3}Se_{0.7}$. Due to the recovery induced n_H-reduction, remarkable improvements in α were obtained with increasing the HD count (Figure S3, Supporting Information). Meanwhile, κ is distinctly reduced owing to the deformation-induced lattice defects (Figure S3, Supporting Information). Consequently, a record value of ZT= 1.2 at 445 K was achieved for the n-type $Bi_2Te_{2.3}Se_{0.7}$ sample hot deformed three times (HD3) with both the thermal and electrical properties measured along the in-plane direction (Figure 4c), which is a 20% increase over the sample hot deformed once (HD1). This is the highest ZT value reported for the n-type Bi_2Te_3 based alloys (Figure 4d). It is noteworthy that the maximum ZT value in this work was close to 2.0, if the in-plane electrical conductivity and out-of-plane thermal conductivity were used to calculate ZT, as generally adopted, leading to a 70% overestimation.

2.2. Ternary p-Type $Bi_ySb_yTe_3$ System

Point defect engineering is also effective in improving the TE performance of p-type Bi_2Te_3 based alloys. Similar to the n-type system, the optimum compositions of p-type polycrystalline $Bi_{2-y}Sb_yTe_3$ should also be different from the single crystals because of the deformation induced donor-like effect.

Raising the Sb content in p-type $Bi_{2-y}Sb_yTe_3$ reduces E_{AS} and thereby increases the hole concentration on account of the smaller differences in electronegativity χ and covalent radius in Sb–Te as compared to Bi–Te.[12,22] The alloy composition $Bi_{0.5}Sb_{1.5}Te_3$ is generally believed to have the optimal hole concentration and the maximum ZT value for unidirectionally grown ingots in the past decades.[26] However, for the polycrystalline samples subjected to powder processing, the hole concentration will be greatly reduced by the

© 2014 WILEY-VCH Verlag GmbH & Co. KGaA, Weinheim

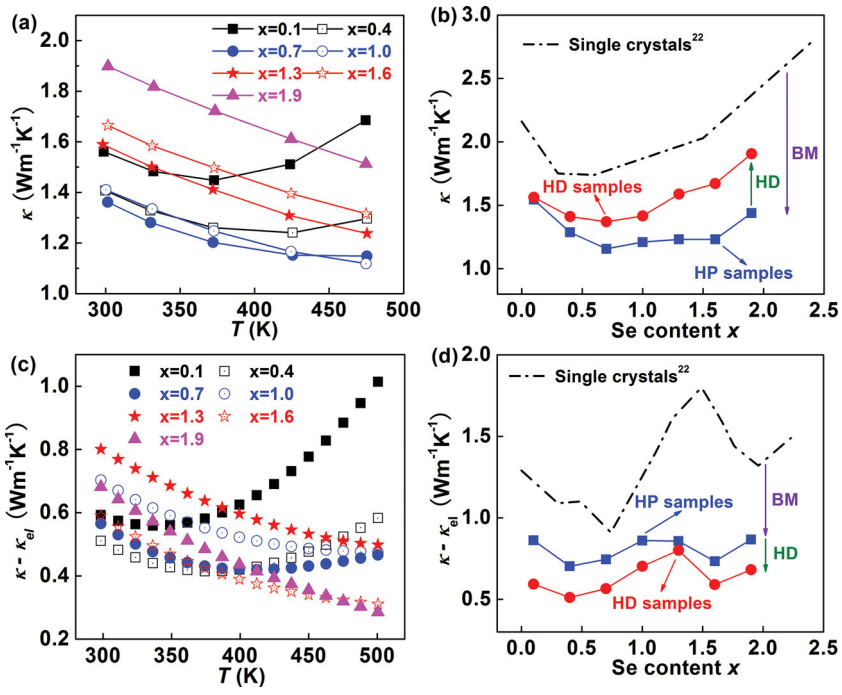

Figure 3. a) Temperature dependence of the in-plane thermal conductivity of the hot deformed $Bi_2Te_{3-x}Se_x$ samples, b) room temperature thermal conductivity of the single crystals,[22] HP and HD $Bi_2Te_{3-x}Se_x$ samples, c) temperature dependence of the in-plane lattice thermal conductivity of the hot deformed $Bi_2Te_{3-x}Se_x$ samples, and d) room temperature lattice thermal conductivity of the single crystals,[22] HP and HD $Bi_2Te_{3-x}Se_x$ samples.

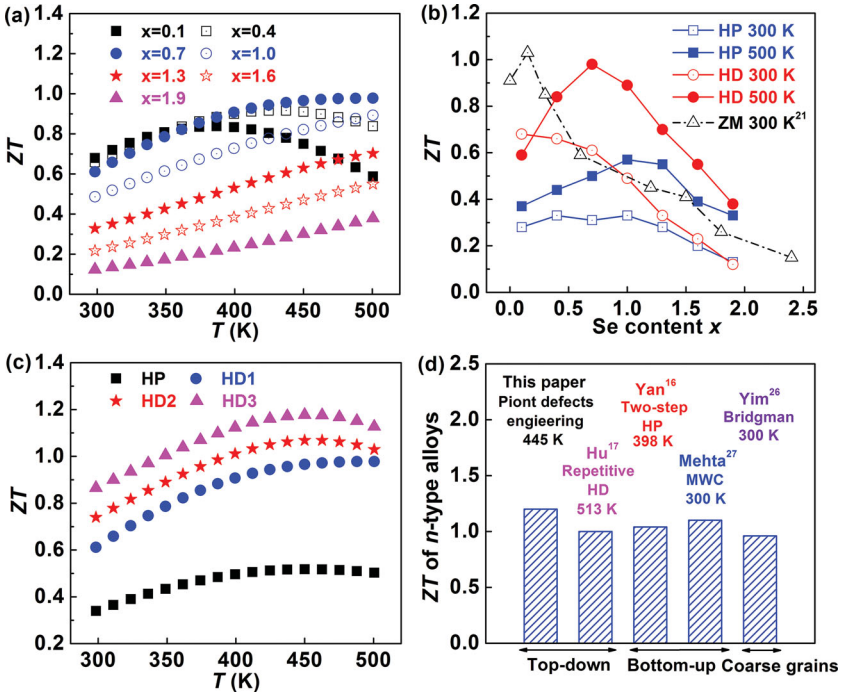

Figure 4. a) Temperature dependence of *ZT* of the hot deformed $Bi_2Te_{3-x}Se_x$ samples. b) Se content dependence of ZT of the ZM,[21] HP and HD $Bi_2Te_{3-x}Se_x$ samples. c) Temperature dependences of *ZT* of the repetitive hot deformed $Bi_2Te_{2.3}Se_{0.7}$ samples. d) Maximum *ZT* compared with other state-of-the-art work.[16,17,26,27]

deformation-induced donor-like effect[15] (**Figure 5**), leading to the deteriorative TE performance. It is obvious that n_H of the polycrystalline sample $y = 1.7$ is nearly equal to that of the $y = 1.5$ single crystal, indicating that the optimal hole concentration in polycrystalline samples can be obtained by raising antisite defects (i.e., Sb'_{Te} and Bi'_{Te}). However, many previous studies on polycrystalline p-type alloys are still based on the optimum composition $y = 1.5$ of single crystals.[1,2] In point defect engineering, it is crucial to elucidate how to tune the point defects in p-type Bi_2Te_3 based alloys by hot deformation. The HD induced donor-like effect partly compensates holes, resulting in a fall in n_H compared to the HP counterparts.[15] Moreover, it is noted that the n_H-reduction is notably weakened with increasing the Sb content (Figure 5). Similar to the n-type $Bi_2Te_{3-x}Se_x$ system, the HD process also enhances the textures and improves μ_H of p-type polycrystalline $Bi_{2-y}Sb_yTe_3$ alloys (Figure S4, Supporting Information).

By optimizing n_H via engineering point defects, good electrical properties have been achieved (**Figure 6**). The substitution of Bi by Sb atoms in the Bi_2Te_3 lattice dramatically improves σ, resulting from the increase in n_H due to the increased antisite defects (Figure S5, Supporting Information). σ of samples $y = 1.6$ and 1.7, rather than the traditional $y = 1.5$, is much closer to the optimum σ of 1.0×10^5 Sm^{-1} at room temperature for the Bi_2Te_3 based alloys. The reduction in σ after BM is the result of the donor-like effect (Figure 6a). Correspondingly, α markedly declines with increasing y (Figure S5, Supporting Information). Polycrystalline samples of $y = 1.6$ and 1.7 exhibit a high α value of ≈200 μVK^{-1} throughout the whole temperature range. The temperature at which the maximum α occurs gradually rises with the Sb content, which is mainly ascribed to the suppressed intrinsic conduction by increasing the hole concentration. Compared to the single crystals, α of the HP and HD samples is improved owing to the decreased n_H induced by the donor-like effect (Figure 6b). Consequently, a maximum *PF* of 4.5×10^{-3} $Wm^{-1}K^2$ was achieved at room temperature for the hot deformed $Bi_{0.3}Sb_{1.7}Te_3$ sample (Figure S6, Supporting Information).

The change of κ in p-type $Bi_{2-y}Sb_yTe_3$ is obviously related to point defects, similar to that of the n-type ones (Figure S7, Supporting Information). Room temperature κ rises with increasing y due to the increased value of

© 2014 WILEY-VCH Verlag GmbH & Co. KGaA, Weinheim

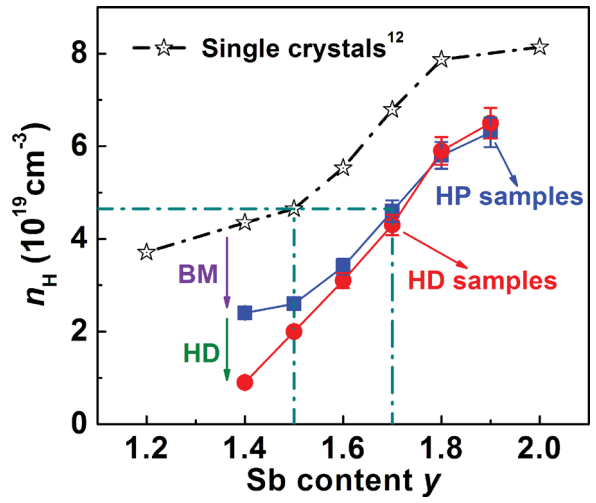

Figure 5. Room temperature carrier concentration of the undoped single crystals,[12] HP and HD $Bi_{2-y}Sb_yTe_3$ samples.

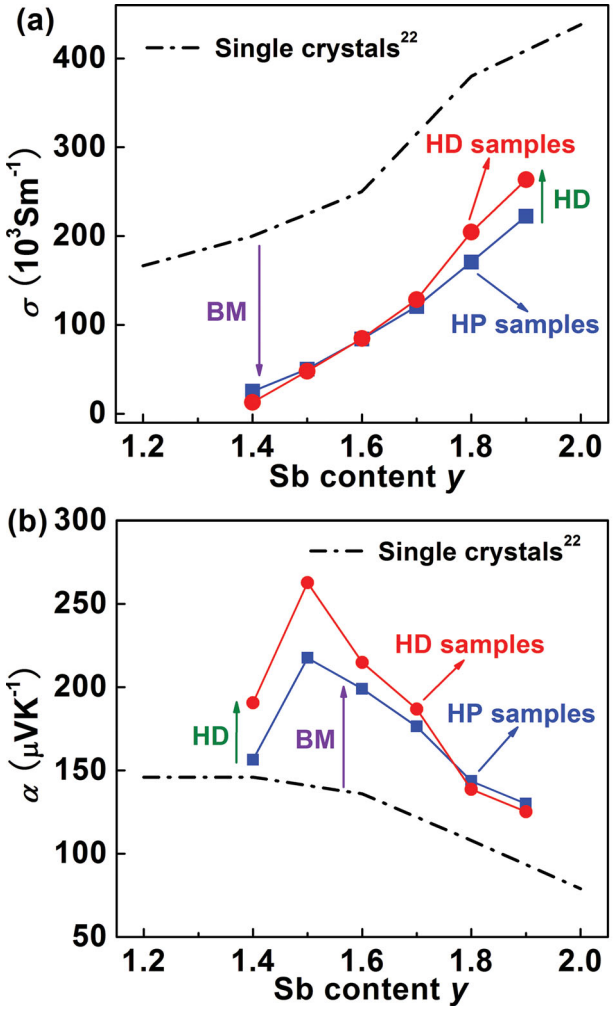

Figure 6. Room temperature in-plane a) electrical conductivity and b) Seebeck coefficient of undoped single crystals,[22] HP and HD $Bi_{2-y}Sb_yTe_3$ samples.

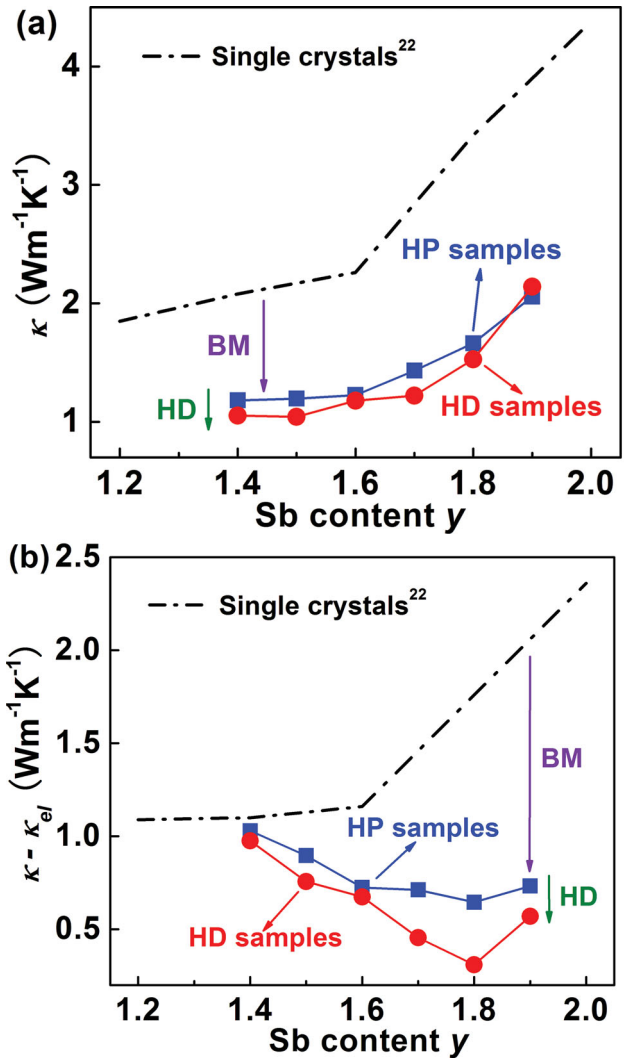

Figure 7. Room temperature in-plane a) total thermal conductivity and b) lattice thermal conductivity of the undoped single crystals,[22] HP and HD $Bi_{2-y}Sb_yTe_3$ samples.

κ_{el}, as shown in **Figure 7**a. κ_{ph} of the HD samples was calculated using the same method as for the n-type alloys (Figure S7, Supporting Information). Figure 7b shows room temperature κ_{ph} of undoped single crystals, HP and HP samples. The generation of V'''_{Sb} (or V'''_{Bi}) and $V^{\cdot\cdot}_{Te}$ during the deformation (Equation (3)) results in a decrease of κ_{ph} for the HP and HD samples. Besides, deformation-induced lattice distortion also contributes to the decline of κ_{ph}.[8,17,20]

By engineering the point defects via optimizing the Sb content and hot deformation, the hot deformed $Bi_{0.3}Sb_{1.7}Te_3$ sample shows the highest $ZT \approx 1.3$ at 380 K (Figure S8, Supporting Information). As compared to the traditionally grown $Bi_{0.5}Sb_{1.5}Te_3$ ingots with a maximum $ZT \approx 1$ near room temperature,[26,28] the optimum composition is shifted to a higher Sb content for the polycrystalline samples owing to the deformation induced donor-like effect (**Figure 8**a). Our result is consistent with the recent work by Li et al., who reported a high ZT value for ball milled $Bi_{0.3}Sb_{1.7}Te_3$ alloys,

© 2014 WILEY-VCH Verlag GmbH & Co. KGaA, Weinheim

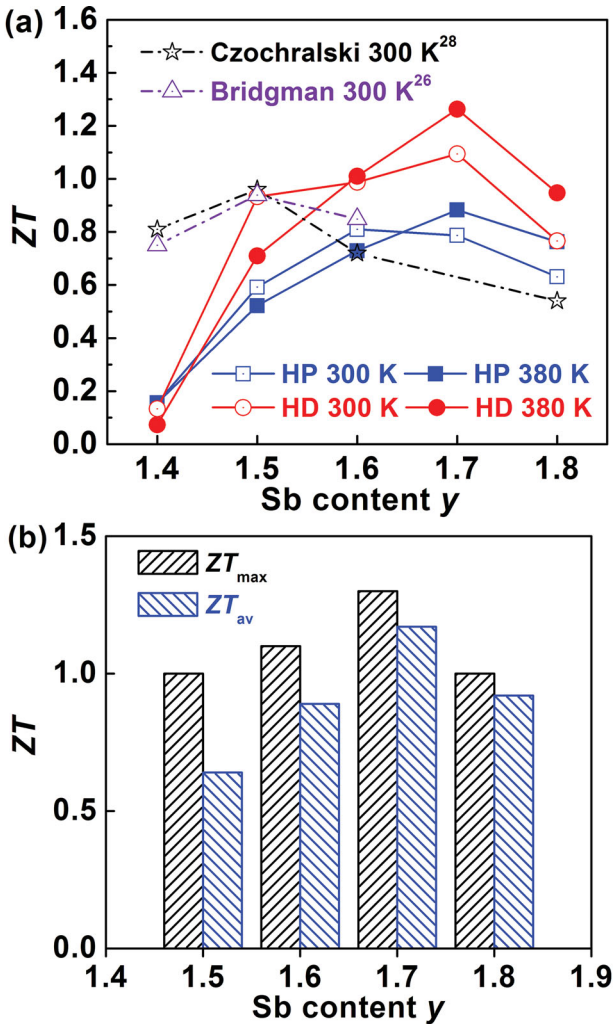

Figure 8. a) Sb content y dependence of ZT values for the traditionally grown ingots,[26,28] HP and HD $Bi_{2-y}Sb_yTe_3$ samples, b) Sb content dependence of ZT_{max} and ZT_{av} of hot deformed $Bi_{2-y}Sb_yTe_3$ samples.

not $Bi_{0.5}Sb_{1.5}Te_3$.[29] Also, there is a significant improvement of the average ZT_{av} throughout the studied temperature range, which is 1.2 for the hot deformed $Bi_{0.3}Sb_{1.7}Te_3$ sample (Figure 8b). It is also worth pointing out that, if the in-plane electrical conductivity and the out-of-plane thermal conductivity were used to determine *ZT*, the figure of merit will be overestimated to be about 1.9.

3. Conclusion

In summary, optimized values of n_H and reduced values of κ_{ph} were obtained by point defect engineering, which allows to design and optimize compositions of both undoped n- and p-type bismuth telluride based TE materials. The results on both n- and p-type bismuth telluride based alloys demonstrate that modulating point defects enables simultaneous improvements in electrical properties and lattice thermal conductivity, leading to enhanced *ZT* values. A record *ZT* value of ≈1.2 at 445 K was obtained for n-type polycrystalline $Bi_2Te_{2.3}Se_{0.7}$ alloys, and a high *ZT* of ≈1.3 at 380 K was also achieved for p-type polycrystalline $Bi_{0.3}Sb_{1.7}Te_3$ alloys, both alloys showing different optimal compositions than conventionally grown ingots. Further development of quaternary or non-stoichimetric alloys by point defect engineering shows great potential for the improvement of *ZT*. We also believe that point defect engineering can play an important role in enhancing the figure of merit of other TE materials.

4. Experimental Section

The commercial high-purity elemental chunks of 99.999% Bi, 99.999% Sb, 99.999% Te, and 99.999% Se were weighed according to the nominal composition of $Bi_2Te_{3-x}Se_x$ (x = 0.1, 0.4, 0.7, 1.0, 1.3, 1.6, and 1.9) and $Bi_{2-y}Sb_yTe_3$ (y = 1.4, 1.5, 1.6, 1.7, 1.8, and 1.9) and sealed into a quartz tube at 10^{-3} Pa. The element mixture was then melted for 10 h in a box furnace at 1073 K and 1023 K for n- and p-type alloys, respectively. Fine powders were made by ball milling (Retsch, MM 200) the obtained ingots for 20 min at 20 and 15 Hz for n- and p-type alloys, respectively.

The as-obtained powders were hot pressed into a cylinder in a ϕ 10 mm graphite die at 673K for 30 min under the uniaxial stress of 80 MPa, producing the initial bulk samples named as HP. Subsequently, a hot deformation process was performed by repressing the HP samples in a larger graphite die with an inner diameter of 16 mm at 823 K for 30 min using the same stress. Finally, disk-shaped samples of 16 mm called HD were obtained.

The actual chemical compositions were characterized by electron probe microanalysis (EPMA, JEOL JXA-8100) with a wave dispersive spectrometer (WDS). The in-plane thermal diffusivity (D) measurements were performed on a Netzsch LFA 457 laser flash apparatus with a Pyroceram standard using the method described in detail in the literature.[20] The specific heat (C_P) was measured on the Netzsch DSC 404C and the density (ρ_D) was estimated by an ordinary dimension and weight measurement procedure. The in-plane thermal conductivity was then calculated using the relation $\kappa = D\rho_D C_P$. The in-plane electrical conductivity (σ) and the Seebeek coefficient (α) were simultaneously measured on a commercial Linseis LSR-3 system. The Hall coefficient (R_H) was determined at 300 K on a Quantum Design PPMS-9T instrument using a four-probe configuration. Then the carrier concentration (n_H) and in-plane Hall mobility (μ_H) were computed according to $n_H = 1/eR_H$ and $\mu_H = \sigma R_H$, respectively.

Supporting Information

Supporting Information is available from the Wiley Online Library or from the author.

Acknowledgements

The work was supported by the National Basic Research Program of China (2013CB632503), the Nature Science Foundation of China (51271165 and 51171171), the Program for New Century Excellent Talents in University (NCET-12-0495), the Program for Innovative Research Team in University of Ministry of Education of China (IRT13037), and the Ph.D program Foundation of Ministry of Education of China (20110101110024).

Received: February 11, 2014
Revised: March 18, 2014
Published online: June 2, 2014

© 2014 WILEY-VCH Verlag GmbH & Co. KGaA, Weinheim

[1] B. Poudel, Q. Hao, Y. Ma, Y. C. Lan, A. Minnich, B. Yu, X. Yan, D. Z. Wang, A. Muto, D. Vashaee, X. Y. Chen, J. M. Liu, M. S. Dresselhaus, G. Chen, Z. F. Ren, *Science* **2008**, *320*, 634.
[2] X. F. Tang, W. J. Xie, H. Li, W. Y. Zhao, Q. J. Zhang, M. Niino, *Appl. Phys. Lett.* **2007**, *90*, 012102.
[3] J. Androulakis, K. F. Hsu, R. Pcionek, H. J. Kong, C. Uher, J. J. DAngelo, A. Downey, T. Hogan, M. G. Kanatzidis, *Adv. Mater.* **2006**, *18*, 1170.
[4] C. J. Vineis, A. Shakouri, A. Majumdar, M. G. Kanatzidis, *Adv. Mater.* **2010**, *22*, 3970.
[5] Y. Z. Pei, J. Lensch-Falk, E. S. Toberer, D. L. Medlin, G. J. Snyder, *Adv. Funct. Mater.* **2011**, *21*, 241.
[6] J. P. Heremans, V. Jovovic, E. S. Toberer, A. Saramat, K. Kurosaki, A. Charoenphakdee, S. Yamanaka, G. J. Snyder, *Science* **2008**, *321*, 554.
[7] Y. Pei, H. Wang, G. J. Snyder, *Adv. Mater.* **2012**, *24*, 6125.
[8] L. P. Hu, H. L. Gao, X. H. Liu, H. H. Xie, J. J. Shen, T. J. Zhu, X. B. Zhao, *J. Mater. Chem.* **2012**, *22*, 16484.
[9] Z. L. Du, T. J. Zhu, Y. Chen, J. He, H. L. Gao, G. Y. Jiang, T. M. Tritt, X. B. Zhao, *J. Mater. Chem.* **2012**, *22*, 6838.
[10] T. Dasgupta, C. Stiewe, R. Hassdorf, A. J. Zhou, L. Boettcher, E. Mueller, *Phys. Rev. B* **2011**, *83*, 235207.
[11] H. H. Xie, Y. Cu, T. J. Zhu, C. G. Fu, G. J. Snyder, X. B. Zhao, *Appl. Phys. Lett.* **2012**, *100*, 254104.
[12] Z. Stary, J. Horak, M. Stordeur, M. Stolzer, *J. Phys. Chem. Solids* **1988**, *49*, 29.
[13] J. Horak, Z. Stary, P. Lostak, J. Pancir, *J. Phys. Chem. Solids* **1990**, *51*, 1353.
[14] D. West, Y. Y. Sun, H. Wang, J. Bang, S. B. Zhang, *Phys. Rev. B* **2012**, *86*, 121201.
[15] J. Navratil, Z. Stary, T. Plechacek, *Mater. Res. Bull.* **1996**, *31*, 1559.
[16] X. Yan, B. Poudel, Y. Ma, W. S. Liu, G. Joshi, H. Wang, Y. C. Lan, D. Z. Wang, G. Chen, Z. F. Ren, *Nano Lett.* **2010**, *10*, 3373.
[17] L. P. Hu, X. H. Liu, H. H. Xie, J. J. Shen, T. J. Zhu, X. B. Zhao, *Acta Mater.* **2012**, *60*, 4431.
[18] R. Ionescu, J. Jaklovszky, N. Nistor, A. Chiculita, *Phys. Status Solidi A* **1975**, *27*, 27.
[19] K. Termentzidis, O. Pokropyvnyy, M. Woda, S. Xiong, Y. Chumakov, P. Cortona, S. Volz, *J. Appl. Phys.* **2013**, *113*, 4431.
[20] J. J. Shen, T. J. Zhu, X. B. Zhao, S. N. Zhang, S. H. Yang, Z. Z. Yin, *Energy Environ. Sci.* **2010**, *3*, 1519.
[21] S. Y. Wang, G. J. Tan, W. J. Xie, G. Zheng, H. Li, J. H. Yang, X. F. Tang, *J. Mater. Chem.* **2012**, *22*, 20943.
[22] U. Birkholz, *Z. Naturforsch. A* **1958**, *13*, 780.
[23] P. Lostak, C. Drasar, D. Bachan, L. Benes, A. Krejcova, *Radiat. Eff. Defects Solid* **2010**, *165*, 211.
[24] L. D. Zhao, B. P. Zhang, J. F. Li, H. L. Zhang, W. S. Liu, *Solid State Sci.* **2008**, *10*, 651.
[25] I. Teramoto, S. Takayanagi, *J. Phys. Chem. Solids* **1961**, *19*, 124.
[26] W. M. Yim, F. D. Rosi, *Solid-State Electron.* **1972**, *15*, 1121.
[27] R. J. Mehta, Y. L. Zhang, C. Karthik, B. Singh, R. W. Siegel, T. Borca-Tasciuc, G. Ramanath, *Nat. Mater.* **2012**, *11*, 233.
[28] L. D. Ivanova, Y. U. Granatkina, *Inorg. Mater.* **1995**, *31*, 678.
[29] J. H. Li, Q. Tan, J. F. Li, D. W. Liu, F. Li, Z. Y. Li, M. M. Zou, K. Wang, *Adv. Funct. Mater.* **2013**, *23*, 4317.

© 2014 WILEY-VCH Verlag GmbH & Co. KGaA, Weinheim